
It's FLAN time! Summing feature-wise latent representations for interpretability

An-phi Nguyen

IBM Research Europe, ETH Zürich
Zürich, Switzerland
uye@zurich.ibm.com

Maria Rodríguez Martínez

IBM Research Europe
Zürich, Switzerland
mrm@zurich.ibm.com

Abstract

Interpretability has become a necessary feature for machine learning models deployed in critical scenarios, e.g. legal system, healthcare. In these situations, algorithmic decisions may have (potentially negative) long-lasting effects on the end-user affected by the decision. In many cases, the representational power of deep learning models is not needed, therefore *simple and interpretable* models (e.g. linear models) should be preferred. However, in high-dimensional and/or complex domains (e.g. computer vision), the universal approximation capabilities of neural networks are required. Inspired by linear models and the Kolmogorov-Arnol representation theorem, we propose a novel class of *structurally-constrained* neural networks, which we call FLANs (Feature-wise Latent Additive Networks). Crucially, FLANs process each input feature *separately*, computing for each of them a representation in a common latent space. These feature-wise latent representations are then simply *summed*, and the aggregated representation is used for prediction. These constraints (which are at the core of the interpretability of linear models) allow a user to estimate the effect of each individual feature *independently* from the others, *enhancing interpretability*. In a set of experiments across different domains, we show how without compromising excessively the test performance, the structural constraints proposed in FLANs indeed increase the interpretability of deep learning models.

1 Introduction

The recent surge in interest towards *interpretable machine learning* research can arguably be attributed to the success of deep learning models. Despite their universal approximation capabilities [1, 2] and generalization properties [3, 4], these models often behave as a black-box from a user perspective: their “decision process” is often unclear, especially to layman users. While not always necessary, interpretability can be *critical* in applications with far-reaching impact, e.g. in legal cases and healthcare. In these high-stake scenarios, Rudin [5] advocates for *simple* and *already interpretable* models. Indeed, for various real-world problems, simple interpretable models perform similarly to more complex models [6] and should therefore be preferred.

Unfortunately, this solution is not applicable for high-dimensional and/or complex problems where the representational capabilities of end-to-end deep learning models give them an edge against other models, e.g. autonomous driving [7] or machine translation [8]. In these cases, interpretability can be achieved in two ways. *Post-hoc* methods, such as feature attribution methods [9], can be leveraged to produce an explanation for a model that *has already been trained*. Alternatively, it is possible to directly train complex *ante-hoc* models, which are models with some kind of “in-built mechanism” that allows for their scrutiny. Classical examples are decision trees [10]. Recently, there has been an increased interest in developing ante-hoc deep learning models that attempt at retaining

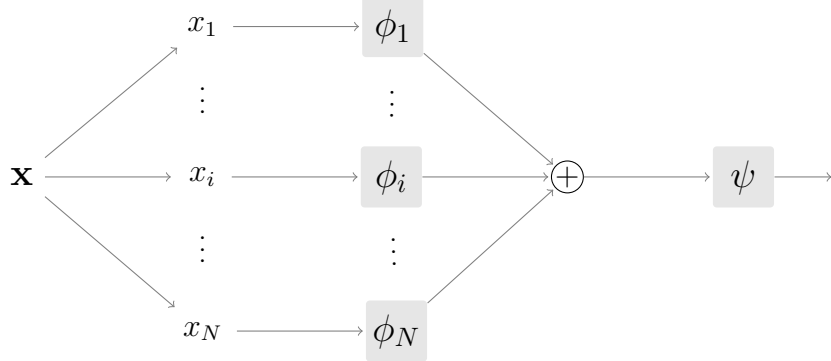


Figure 1: The base architecture of FLANs. A sample \mathbf{x} is split in its features x_i . Each of the feature is fed to a different function ϕ_i . All the processed features are then aggregated by summation, and finally fed to a prediction network ψ . In our work, all the functions ϕ_i and ψ are implemented as neural networks.

the representational and generalization properties of neural networks, whilst still being interpretable (e.g. [11, 12, 13]).

In this paper, we introduce a model, which we denote *FLAN* (Feature-wise Latent Additive Network), that belongs to this last class of interpretable models. Inspired by linear models, FLAN computes a latent representation of each feature (or subsets thereof) *separately*. The latent representation of an input sample is obtained by simply *summing* the feature representations, and then passed to a classifier network for classification. We posit that these two constraints are what enables the interpretability of our model (Section 2.1). Despite these constraints, our model can still achieve good performance on a series of benchmark tasks in different domains.

2 FLANs

2.1 Interpretability lessons from linear models

Linear models are generally considered among the prime examples of interpretable models. Arguably this is due to two key characteristics of these models:

- *Separability of features*: Linear models do not take *interactions* among features into account (unless an interaction term is explicitly added to the features). This means that a user can examine the effect of each feature *separately* from the others. This, in turn, makes the model easier to understand from a user perspective [14];
- *Predictability of the output*: Given a single feature, its effect on the output can be easily understood by a human user if the relationship is linear [15]. In the presence of multiple features, the human can still easily predict their effect on the output(s), if their effect is separable as discussed in the previous point.

2.2 Model Architecture

Motivated by the previous section, we want to build a model for which the effect of single features can be predicted separately from each other. Let us assume that our goal is to learn a function $f : \mathcal{X} \rightarrow \mathcal{Y}$, where \mathcal{X} has dimension N and \mathcal{Y} has dimension M . We propose to implement the function f as:

$$f(\mathbf{x}) = f(x_1, \dots, x_i, \dots, x_N) = \psi \left(\sum_{i=1}^N \phi_i(x_i) \right) \quad (1)$$

where:

- x_i (with $i = 1, \dots, N$) are the features, i.e. the components of the input sample \mathbf{x} ;

- $\phi_i : \mathcal{X}_i \rightarrow \mathcal{Z}$ are feature functions that act on each individual feature x_i separately and map them to the *same* latent space \mathcal{Z} of dimension D . Note that the feature functions may either implement different functions, or the same function for all features;
- the aggregate $\sum_{i=1}^N \phi_i(x_i) = \mathbf{z} \in \mathcal{Z}$ is the latent representation for the input sample \mathbf{x} ;
- the predictor function $\psi : \mathcal{Z} \rightarrow \mathcal{Y}$ maps the sample latent representation to the output space \mathcal{Y} .

In this paper, we implement the feature functions ϕ_i and the prediction function ψ as neural networks and learn them in an end-to-end fashion. Figure 1 provides a depiction of our model.

Before discussing the interpretability of our model (Section 2.3), we would like to make a few remarks.

Remark 2.2.1 (Universal Approximation). Since no interaction is explicitly modeled in Eq. (1), a concern that may be raised is if our model still retains the same approximation capabilities of traditional neural networks. The answer is given by the *Kolmogorov-Arnol representation theorem* [16] which claims, informally, that any continuous function of a finite number of variables can be expressed in the form

$$f(\mathbf{x}) = f(x_1, \dots, x_N) = \sum_{q=0}^{2N} \Phi_q \left(\sum_{i=1}^N \phi_{q,i}(x_i) \right)$$

Note that for interpretability purposes, we do not need the outer sum since it would not separate neither the outputs nor the effects of the input features. We therefore use a more generic function ψ . The strength of the Kolmogorov Arnol representation theorem is in claiming that there is actually *no need* to explicitly model interactions. Although there is some debate about the applicability of the Kolmogorov-Arnol theorem (e.g. [17] vs [18]), in Section 4 we experimentally show that our model can (over)fit the training dataset.

Remark 2.2.2 (Feature subgroups). In some applications, having a function applied to each individual feature may be detrimental. From an interpretability perspective, this is especially true when a single feature has no particular meaning. For example, consider computer vision tasks: human users rarely understand image classification in terms of single pixels, but rather in terms of higher-level concepts. Eq. (1) can be adapted to consider features in (*non-overlapping*) *groups* rather than individually. Building on the computer vision example, an image could be processed in *patches* rather than single pixels.

Remark 2.2.3 (Structural information). Some data types carry additional structural information, e.g. natural language or images. Eq. (1) can be applied directly also to these domains. However, for the purpose of parameter sharing, it may be useful to make the dependency on the structure explicit:

$$f(\mathbf{x}) = f(x_1, \dots, x_N) = \psi \left(\sum_{i=1}^N \phi(x_i; \theta, p_i) \right)$$

where θ are parameters common to all the feature functions, and p_i encode some kind of structural information. This is the same idea behind the positional embeddings used in Transformer architectures [19].

Remark 2.2.4 (Parallel inference). While the training may need to be performed jointly for all the feature functions, at inference they can be applied in parallel. This is particularly useful for those scenarios where even a single sample of the dataset may be relatively big. An example is represented by digital pathology data, where a single sample may occupy a few thousands megabytes on disk [20].

Remark 2.2.5 (Other use cases for FLANs). While our work is motivated by interpretability, our model could be apt for other settings. For example, when we deal with *missing/corrupted* data, a common strategy is data imputation [21, 22]. In our model, this is not necessary: since all the feature functions ϕ_i map to the same latent space, the prediction network ψ can be applied regardless of the number of features included. This means that, if we are dealing with a missing feature, we can just omit it from the sum. Another use case where our model can be trivially extended is given by *multimodal* data: a different feature function can be learned for each data modality.

2.3 Interpreting FLANs

In this section, we will discuss the three main modalities to interpret FLANs. Concrete examples will then be presented in Section 4.

2.3.1 Separating and predicting the effect of *individual* features

The interpretability of FLANs stems from the fact that different features are processed *separately*. That is, we can analyze how each feature contributes to the prediction without being concerned about interactions.

As discussed in Remark 2.2.5, the prediction network ψ can be applied regardless of the number of features used. Consequently, a user can study the effect of a single feature x_i simply by performing a prediction on that feature, i.e. $\psi(\mathbf{z}_i)$ with $\mathbf{z}_i = \phi_i(x_i)$. Note however that, since we are not making any assumption on the function ψ , the effect is not generally additive. In fact, assume that \mathcal{Y} and \mathcal{Z} are equipped, respectively, with norms $\|\cdot\|_{\mathcal{Y}}$ and $\|\cdot\|_{\mathcal{Z}}$. Further, let us informally assume that we can compute the Taylor expansion of ψ in a “large enough” neighborhood of $\mathbf{z}_* = \sum_{j=1, j \neq i}^N \mathbf{z}_j$. Then we have

$$\left\| \underbrace{\psi(\mathbf{z}_* + \mathbf{z}_i) - \psi(\mathbf{z}_*)}_{(\Delta)} - \psi(\mathbf{z}_i) \right\|_{\mathcal{Y}} = \|\mathbf{J}_{\mathbf{z}_*} \mathbf{z}_i - \psi(\mathbf{z}_i) + o(\|\mathbf{z}_*\|_{\mathcal{Z}})\|_{\mathcal{Y}} \quad (2)$$

where:

- $\psi(\mathbf{z}_* + \mathbf{z}_i) - \psi(\mathbf{z}_*)$ is the change in prediction given by the additional information contained in the i -th feature;
- $\mathbf{J}_{\mathbf{z}_*}$ is the Jacobian of ψ computed at point \mathbf{z}_* ;
- $o(\|\mathbf{z}_*\|_{\mathcal{Z}})$ is the remainder term in the first-order Taylor expansion.

The right-hand side of Eq. (2) gets closer to zero the “more linear” is ψ . Therefore Eq. (2) is telling us that we can estimate the change in prediction (Δ) given by feature i by looking at the prediction $\psi(\mathbf{z}_i)$ on that feature. The accuracy of the estimation will depend on how non-linear is ψ . Although, we are not making any assumption on ψ , in Section 4.2 we show that in practice we can still estimate the effect of single features on the prediction.

2.3.2 Feature importance

The interpretability modality described in the previous section has mostly an “algorithmic/mechanistic” flavor. However, FLANs can be interpreted also by computing feature importances without the need for *post-hoc* methods, such as SHAP [23]. Since sample representations are simply the *sum* of feature representations, then a feature i that is mapped to a small vector $\|\mathbf{z}_i\|_{\mathcal{Z}} \approx 0$ brings no contribution to the prediction. This means that we can use the norms of the feature latent representations as indicative of feature importance.

2.3.3 Example-based

FLANs can be further interpreted via examples/prototypes: to interpret the model at an input sample $\hat{\mathbf{z}}$, we only need to look for the nearest samples $\tilde{\mathbf{z}}$ in the latent space. Since ψ in our model is a neural network, and therefore a Lipschitz continuous function, i.e. $\|\psi(\hat{\mathbf{z}}) - \psi(\tilde{\mathbf{z}})\|_{\mathcal{Y}} \leq L\|\hat{\mathbf{z}} - \tilde{\mathbf{z}}\|_{\mathcal{Z}}$, the predictions performed on two samples with similar representations will be similar.

This analysis can be performed also on a feature level. That is, by looking for features with similar representations, we can understand which features provide similar information towards the prediction. Similarly, by looking at *dissimilar* features, we are able to understand why two samples may be classified differently.

3 Related Work

Our work is motivated by interpretability. In the taxonomy [24] of interpretability methods, FLANs classifies primarily as a *local* method since the model can be explained at single sample points. A more *global* overview of the model can be obtained by looking for similar samples in the latent space, as explained in Section 2.3.3. Here, any of previously proposed methods can be used (e.g. MMD-Critic [25], ProtoDash [26]).

FLANs can be inspected also via feature attributions (Section 2.3.2). These feature importances are computed as norms of the feature representations. Therefore there is no need to use any post-hoc

method, such as gradient-based methods [9, 27, 28, 29] or SHAP [23], which would require more computational resources. This advantage is shared with Transformer models [19], where the attention scores can be interpreted as importances. However, the attention scores are function of *all* the feature, effectively modeling interactions. This, in turn, decreases separability and, consequently, interpretability.

From a modeling perspective, FLANs belong to the class of *ante-hoc structurally constrained* deep learning models. Notable methods in this category are those that augment the network with prototype/prototypical-part based reasoning, e.g. [11, 30]. A similar mechanism can be achieved also with FLANs (Section 2.3.3) without the need of an *ad-hoc* cost function or training strategy. Prototypes are similar in spirit to the concepts/feature basis used in Self-Explaining Neural Networks (SENNs) [12]. Interestingly, Alvarez Melis and Jaakkola [12] also recognize the value of additivity/separability for interpretability. However, additivity is enforced only in the last layer in their model. The concepts (and their relevances) are computed as functions of the entire input space. Consequently, the interpretability with respect to the original input space is lost.

Closer in spirit to our model are the neural additive models [31], Explainable Boosting Machines (EBM) [32], and the generalized additive models with interactions [33]. However, these previous works do not leverage a second prediction function after aggregating the per-feature functions, thus potentially losing the approximation capabilities of FLANs. Moreover, the authors demonstrate their model only on tabular datasets, while we show that additivity-based models can be successfully used also in other more complex domains.

4 Experimental results

4.1 FLAN benchmarking results

Datasets. We test FLANs on a series of benchmark datasets across different domains. In the tabular domain, we consider ProPublica’s Recidivism Risk score prediction dataset (COMPAS)¹, and different risk datasets from the UCI benchmark repository [34] (heart,adult,mammo). For image classification, we benchmark FLANs on the two standard digit classification datasets MNIST [35] and SVHN [36], and the fine-grained bird recognition task CUB-200-2011 [37]. Finally, we test FLANs on the text classification datasets AGNews [38] and IMDb [39]. The results are summarised in Table 1. Note that while we use only classification datasets, FLANs can be used for regression tasks as well.

Models for comparison and training. We compare FLANs to both established and state-of-the-art methods. The chosen models for each domain are reported in Table 1. For tabular datasets, we train all the models ourselves. For the other tasks, we only train FLANs and retrieve the performance of other models from the literature. Training details (Appendix A) and further results (Appendix B) are provided in the appendix. However, it is important to specify how FLANs splits the features in each task. For tabular tasks, FLANs simply process each feature individually. Similarly, in text datasets, our model considers each token in the sentence as a single feature. For image datasets, *non-overlapping* square patches are the features fed to FLANs (Remark 2.2.2).

Tabular datasets results. For benchmarking on tabular datasets, we follow Agarwal et al. [31] and measure the performance of different models in terms of Area Under the Curve (AUC). Table 1a shows that these datasets are easy enough that a simple logistic regression model [41] can perform well. The results on the *adult* and *mammo* datasets suggest that linearity is a good inductive bias for these tasks since logistic regression is able to consistently outperform all the other (non-linear) models. On the other hand, in the *heart* dataset and, to a lesser degree, in the *COMPAS* dataset, it seems beneficial to include non-linearities and interactions. In particular, FLANs closely replicates the performance of more traditional feedforward networks (MLP). This might suggest that FLANs are similar to MLPs in terms of approximation capabilities.

Image datasets results. FLANs results (Table 1b) on the MNIST dataset are comparable to established methods. Moreover, linear models (results not reported) do not achieve more than 94% test accuracy, providing further evidence to the ability of FLANs in implementing interactions *without explicitly modeling them*. We further tested our model on the more difficult fine-grained image

¹<https://github.com/propublica/compas-analysis/>

Table 1: Benchmarking results. (*) denotes pretrained models or models using automated augmentation strategies (e.g. [40]). (**) denotes FLAN models that use pretrained models as *part* of the feature functions.

(a) Area under the curve (AUC) on tabular datasets.				
	COMPAS	adult	heart	mammo
Logistic Regression [41]	0.905	0.892	0.873	0.841
Decision Tree (small) [10]	0.903	0.865	0.849	0.799
Decision Tree (unrestricted) [10]	0.902	0.813	0.848	0.801
Random Forest[42]	0.915	0.869	0.945	0.822
EBM [32]	0.911	0.893	0.941	0.840
MLP	0.915	0.874	0.937	0.831
SENN [12]	0.910	0.865	0.881	0.834
FLAN	0.914	0.880	0.950	0.832

(b) Test accuracy (%) on image datasets.			(c) Test accuracy (%) on text datasets.	
	MNIST	SVHN	CUB	
ResNet [43, 44, 45]	99.2	94.5*	84.5*	
iCaps [44]	99.2	92.0	-	
ViT [45, 46]	-	88.9	90.4*	
ProtoPNet [11]	-	-	84.8*	
SENN [12]	99.1	-	-	
Sota [40, 45, 47]	99.84	99.0*	91.3*	
FLAN	99.05	93.17	70.55**	

classification dataset CUB-200-2011. FLANs do not achieve the same accuracy as other models. This might be explained by the fact that the models reported are pretrained on ImageNet [54] and further fine-tuned on this dataset. On the other hand, in our experiments, our top-performing models use only *some layers* of a pretrained ResNeXt [55] as part of the patch feature function ϕ_i . We hypothesize that the inferior performance of FLANs is attributed to the fact that our model has to essentially *learn the interactions from scratch*, and CUB-200-2011 might be a too small of a dataset to effectively learn this. Despite the lower accuracy, and given the relatively small size of the dataset (11.7k images split across 200 classes), we see our results as promising and a good basis for future investigations in *large scale* image recognition tasks that require interpretability.

Text datasets results. On the considered benchmark datasets, FLANs fair well against traditional LSTM/CNN-based models. The drop in performance of FLANs is particularly noticeable on the IMDb against more modern attention-based architectures. Considering that IMDb contains much longer sentences than AGNews, these results suggest that FLANs may have difficulties in learning longer term dependencies/interactions. This is consistent with the conclusion reached on image datasets.

Summary. FLANs managed to achieve results comparable to the most established models on a series of benchmark datasets. Results against more recent architectures suggest that FLANs may have difficulties in learning complex/long interactions. However, it is worth noting that FLANs do manage to achieve 100% training accuracy in our experiments (Appendix B). This suggests that our model is able to learn complex interactions, although they may not be *generalizable*.

4.2 Interpretability results

4.2.1 COMPAS

We use the COMPAS dataset as a propedeutic example to show how to interpret FLANs. As discussed in Section 2.3.1, we can study the approximate effect of single features separately, by applying the prediction network ψ to the feature latent representation. In this case study, this is even easier

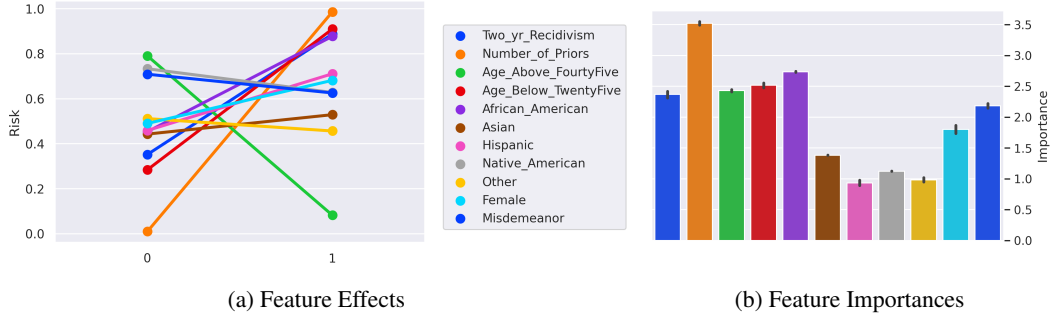


Figure 2: Interpreting a FLAN model trained on the COMPAS dataset. (a) Effect of the single features. (b) Feature importances averaged over the training set. The legend in the center shows the colors used to denote each feature.

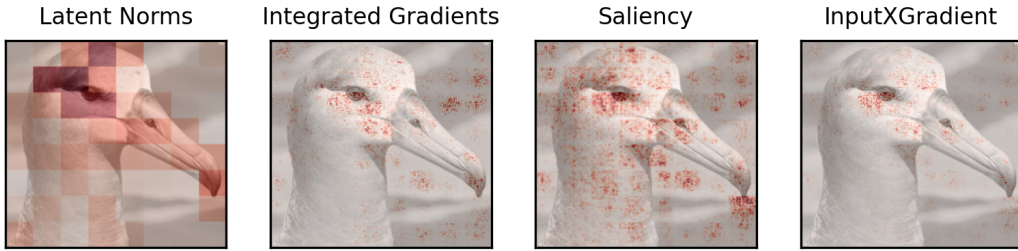


Figure 3: Comparison of the feature importances computed by our model (Latent Norms) against 3 established gradient-based feature attribution methods.

since all the features are binarized. Figure 2a shows how the predicted risk changes if we switch a feature from 0 to 1. The results suggest that the risk is *increased* for criminals that have a high number of priors, are younger than 25, are Afro-American, or have already re-offended in the past two years. Interestingly, the risk seems particularly decreased for criminals above the age of 45. To further validate these findings we analyze the feature importances provided by our model. For each sample, we compute the importances as explained in Section 2.3.2 and then we average them over the training set. Figure 2b confirms that across the training set, the features mentioned above are the most discriminative ones. Previous analyses performed using interpretable models [12, 31] reached similar conclusions.

4.2.2 CUB

We further validate the interpretability capabilities of our model on the more complex CUB-200-2011 dataset.

Feature Importances. We start by comparing the feature importances natively provided by FLANs against three gradient-based *post-hoc* feature attribution methods: Integrated Gradients [29], Saliency [56], and InputXGradient [57]. Figure 3 shows the importances computed by the aforementioned methods for a test sample correctly predicted as a Black Footed Albatross. The norms of the latent representations (Section 2.3.2) highlight features that are typically used to identify birds, i.e. the region around the eye and the beak [11]. While noisier, gradient-based methods highlight some of the same regions, partially validating our model. However, IntegratedGradients and Saliency also highlight some areas in the top-right part of the image. In the next paragraph, we argue that these regions might be indicative of *counterfactual* evidence, rather than “direct” evidence.

Algorithmic interpretation. To show that the top-right area of the image is not particularly important towards the prediction of the sample at hand, we leverage the algorithmic interpretation modality described in Section 2.3.1. More precisely, we drop from the inner sum of Eq. (1) those features with the smallest latent norm. This is shown in Figure 4 (left). Note that this is different from



Figure 4: Algorithmic interpretation of FLANs. In the leftmost image, we show the top 20 most important patches for a Black Footed Albatross. On top of the image we report the top 3 predicted classes (with probabilities) computed on the shown partial image. For reference, we provide also the prediction on the full image and the true label. In the 3 rightmost images we show the top 3 most important patches, together with the top 3 predictions for each of them.

occluding the image [58], which would correspond to imputing values (Remark 2.2.5). As shown at the top of Figure 4 (left), the incomplete image is still classified as Black Footed Albatross. This makes sense since, as argued in Section 2.3.2, features with small norm do not contribute to the sample representation and, consequently, to the prediction. This confirms that the top-right area is not important as direct evidence towards Black Footed Albatross. Rather it may be an area that, if modified, it may *become* important towards a different classification, i.e. a counterfactual.

To further demonstrate the usefulness of separability towards interpretability, we note that the incomplete image has a 10% chance to be classified as Black Billed Cuckoo. To see why it may be, we can apply the prediction network on the single patches. The 3 rightmost images in Figure 4 show how the top 3 patches are classified. In particular, we note that the first and third patch provide evidence towards Black Billed Cuckoo.

Example-based explanations. We finally show the third modality for interpreting FLANs, i.e. by examples. As discussed in Section 2.3.3, to do this we need to look for the nearest neighbors in the latent space \mathcal{Z} before the prediction network. While it can be argued that any layer in the prediction network can be used as a sample representation for nearest neighbor search, we argue that the representation before the prediction network is the most representative of the sample. This is because this is the first point where the information from all the features is aggregated, and no further processing has been performed yet (cf. data processing inequality [59]). Figure 5 shows the bird (center) that most closely resembles the reference Black Footed Albatross (left). In particular, for these images, the top 3 classes predicted are the same (reported on top of the images). However, it can be noted that the computed probabilities for each of these classes are different for the two birds. This means that the two images contain somewhat different information. It is then reasonable to wonder what information do the two images have in common, i.e. why are these two images similar? This can be an important question for assessing similarity models [60]. Informally, we can reformulate this question in the following way. Given the top K features of a sample \mathbf{x} , we would like to find the L features in the second sample $\hat{\mathbf{x}}$ that most closely match them. Mathematically,

$$\min_{S \subset \{1 \dots N\}, |S|=L} \left\| \sum_{i \in T} \mathbf{z}_i - \sum_{j \in S} \hat{\mathbf{z}}_j \right\| \quad (3)$$

where T (with $|T| = K$) is the set of the top K features \mathbf{z}_i of sample \mathbf{x} , and S is any subset of $\{1 \dots N\}$ of cardinality L . To simplify the problem, we restrict L to be equal to K . We further leverage the triangle inequality to split the norm of the sum in a sum of norms. We therefore end up with the following *linear assignment problem* [61] with assignment function $A : T \rightarrow \{1, \dots, N\}$:

$$\min_A \sum_{i \in T} \left\| \mathbf{z}_i - \hat{\mathbf{z}}_{A(i)} \right\| \quad (4)$$

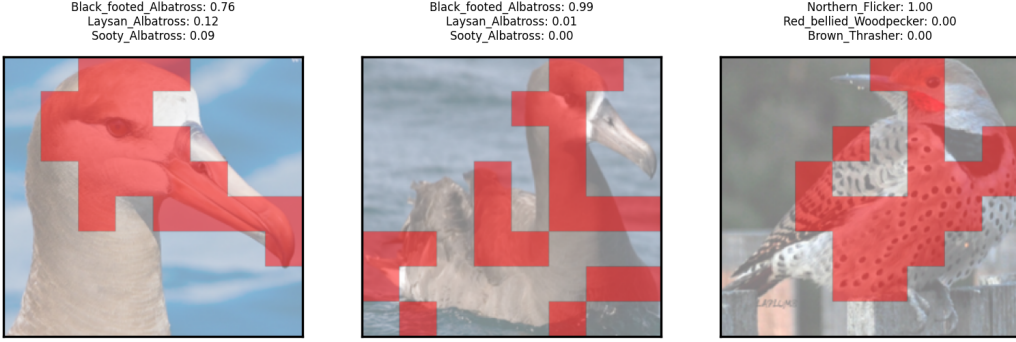


Figure 5: Example-based interpretation of FLANs. (Left) Reference image. (Center) Closest image in the latent space. (Right) Farthest image in the latent space. Above each image, we report the top 3 predicted classes (with probabilities). We highlight in red the patches that explain *why* the center (resp. right) image is close (resp. far) from the reference image.

The red patches in the central image of Figure 5 are the patches assigned to the top features of the reference image on the left. These results show that, again, the eyes of a bird are a distinctive feature. In particular, this feature seems to drive the similarity between the two images.

All the example-based analysis discussed above can be adapted to find and analyze the most *dissimilar* samples. For example, the rightmost image in Figure 5 shows how both the eyes and the feathers are used to distinguish the **Black Footed Albatross** from the **Northern Flicker**.

5 Discussion

FLAN: a powerful interpretable model. Our performance results (Section 4.1) show that FLANs may present generalization difficulties in complex domains. On the other hand, they also suggest that our model is indeed capable of learning any function. In Section 4.2, we demonstrate how easily and natively we can understand the model. Our model is therefore a viable solution for those scenarios where *both* representational power on complex domains and interpretability are required.

Interpretability for different types of users. Miller [62] advocated for a more human-centered design of interpretable methods. In particular, he pointed out that explanations are usually *contextual* in the sense that they should take into account the background and concerns of the user. This means that explanations need to be *personalised* [63, 64]. In Section 4.2, we showed how FLANs can natively be interpreted in 3 different ways, meaning that our model can cater to different types of users depending on their interpretability needs.

Healthcare: an ideal playground for FLANs? In the remarks in Section 2.2, we discussed various scenarios where FLANs may be particularly useful. Healthcare covers all these scenarios. Indeed, in this field, “data-driven practitioners” have to deal with big data (e.g. digital pathology [20], genome sequencing²), missing data [65, 66, 67] and multi-modal data [68]. Considering the importance of interpretability in this field [69], healthcare seems to be the ideal use case scenario for FLANs.

6 Conclusion

In this paper, we introduced a class of *powerful and interpretable* models, which we call FLAN. Our experimental results show that, while our model can achieve reasonable performance on complex datasets, they can still be easily interpreted. We believe that our work represents an important contribution towards interpretable machine learning in *complex domains* with profound societal impact, especially healthcare. In future work, we plan to address the generalization difficulties of our model. Moreover, we plan to run user studies to further validate the interpretability of our model.

²https://www.ridom.de/u/WGS_Data_Types_&_Sizes_and_Runtimes.html

References

- [1] G. Cybenko. Approximation by superpositions of a sigmoidal function. *Mathematics of Control, Signals, and Systems*, 2(4):303–314, 12 1989. ISSN 09324194. doi: 10.1007/BF02551274. URL <https://link.springer.com/article/10.1007/BF02551274>.
- [2] Kurt Hornik, Maxwell Stinchcombe, and Halbert White. Multilayer feedforward networks are universal approximators. *Neural Networks*, 2(5):359–366, 1 1989. ISSN 08936080. doi: 10.1016/0893-6080(89)90020-8.
- [3] Kenji Kawaguchi, Leslie Pack Kaelbling, and Yoshua Bengio. Generalization in Deep Learning. *arXiv*, 10 2017. URL <http://arxiv.org/abs/1710.05468>.
- [4] Sanjeev Arora, Rong Ge, Behnam Neyshabur, and Yi Zhang. Stronger generalization bounds for deep nets via a compression approach. In *35th International Conference on Machine Learning, ICML 2018*, pages 390–418, 2018.
- [5] Cynthia Rudin. Stop explaining black box machine learning models for high stakes decisions and use interpretable models instead. *Nature Machine Intelligence*, 1(5):206–215, 5 2019. doi: 10.1038/s42256-019-0048-x.
- [6] Lesia Semenova, Cynthia Rudin, and Ronald Parr. A study in Rashomon curves and volumes: A new perspective on generalization and model simplicity in machine learning. *arXiv*, 8 2019. URL <http://arxiv.org/abs/1908.01755>.
- [7] Abhishek Gupta, Alagan Anpalagan, Ling Guan, and Ahmed Shaharyar Khwaja. Deep learning for object detection and scene perception in self-driving cars: Survey, challenges, and open issues. *Array*, 10:100057, 7 2021. ISSN 25900056. doi: 10.1016/j.array.2021.100057.
- [8] Yonghui Wu, Mike Schuster, Zhifeng Chen, Quoc V. Le, Mohammad Norouzi, Wolfgang Macherey, Maxim Krikun, Yuan Cao, Qin Gao, Klaus Macherey, Jeff Klingner, Apurva Shah, Melvin Johnson, Xiaobing Liu, Łukasz Kaiser, Stephan Gouws, Yoshikiyo Kato, Taku Kudo, Hideto Kazawa, Keith Stevens, George Kurian, Nishant Patil, Wei Wang, Cliff Young, Jason Smith, Jason Riesa, Alex Rudnick, Oriol Vinyals, Greg Corrado, Macduff Hughes, and Jeffrey Dean. Google’s Neural Machine Translation System: Bridging the Gap between Human and Machine Translation. 9 2016. URL <http://arxiv.org/abs/1609.08144>.
- [9] Marco Ancona, Enea Ceolini, Cengiz Oztireli, and Markus Gross. Towards better understanding of gradient-based attribution methods for Deep Neural Networks. In *6th International Conference on Learning Representations (ICLR 2018)*, 2018.
- [10] J. R. Quinlan. Induction of decision trees. *Machine Learning*, 1(1):81–106, 3 1986. ISSN 0885-6125. doi: 10.1007/bf00116251. URL <https://link.springer.com/article/10.1007/BF00116251>.
- [11] Chaofan Chen, Oscar Li, Daniel Tao, Alina Barnett, Cynthia Rudin, and Jonathan K Su. This Looks Like That: Deep Learning for Interpretable Image Recognition. In H Wallach, H Larochelle, A Beygelzimer, F d Alché-Buc, E Fox, and R Garnett, editors, *Advances in Neural Information Processing Systems 32*, pages 8930–8941. Curran Associates, Inc., 2019. URL <http://papers.nips.cc/paper/9095-this-looks-like-that-deep-learning-for-interpretable-image-recognition.pdf>.
- [12] David Alvarez Melis and Tommi Jaakkola. Towards Robust Interpretability with Self-Explaining Neural Networks. In S Bengio, H Wallach, H Larochelle, K Grauman, N Cesa-Bianchi, and R Garnett, editors, *Advances in Neural Information Processing Systems 31*, pages 7775–7784. Curran Associates, Inc., 2018. URL <http://papers.nips.cc/paper/8003-towards-robust-interpretability-with-self-explaining-neural-networks.pdf>.
- [13] A.-P. Nguyen and M.R. Martínez. MonoNet: Towards Interpretable Models by Learning Monotonic Features, 2019.

[14] Eric Schulz, Joshua B. Tenenbaum, David Duvenaud, Maarten Speekenbrink, and Samuel J. Gershman. Compositional inductive biases in function learning. *Cognitive Psychology*, 99: 44–79, 12 2017. ISSN 00100285. doi: 10.1016/j.cogpsych.2017.11.002.

[15] Eunhee Byun. Interaction between prior knowledge and type of nonlinear relationship on function learning. *Theses and Dissertations Available from ProQuest*, 1 1995. URL <https://docs.lib.psu.edu/dissertations/AAI9622674>.

[16] Andrei Nikolaevich Kolmogorov. On the representation of continuous functions of many variables by superposition of continuous functions of one variable and addition. In *Doklady Akademii Nauk*, volume 114, pages 953–956, 1957.

[17] Federico Girosi and Tomaso Poggio. Representation Properties of Networks: Kolmogorov’s Theorem Is Irrelevant. *Neural Computation*, 1(4):465–469, 12 1989. ISSN 0899-7667. doi: 10.1162/neco.1989.1.4.465.

[18] Věra Kůrková. Kolmogorov’s Theorem Is Relevant. *Neural Computation*, 3(4):617–622, 12 1991. ISSN 0899-7667. doi: 10.1162/neco.1991.3.4.617. URL <http://direct.mit.edu/neco/article-pdf/3/4/617/812230/neco.1991.3.4.617.pdf>.

[19] Ashish Vaswani, Noam Shazeer, Niki Parmar, Jakob Uszkoreit, Llion Jones, Aidan N. Gomez, Łukasz Kaiser, and Illia Polosukhin. Attention is all you need. In *Advances in Neural Information Processing Systems*, volume 2017-December, pages 5999–6009. Neural information processing systems foundation, 6 2017. URL <https://arxiv.org/abs/1706.03762v5>.

[20] Gonzalo Romero Lauro, William Cable, Andrew Lesniak, Eugene Tseytlin, Jeff McHugh, Anil Parwani, and Liron Pantanowitz. Digital pathology consultations - A new era in digital imaging, challenges and practical applications. *Journal of Digital Imaging*, 26(4):668–677, 8 2013. ISSN 08971889. doi: 10.1007/s10278-013-9572-0. URL [/pmc/articles/PMC3705002/](https://pmc.ncbi.nlm.nih.gov/pmc/articles/PMC3705002/)?report=abstracthttps://www.ncbi.nlm.nih.gov/pmc/articles/PMC3705002/.

[21] Donald B. Rubin. Inference and Missing Data. *Biometrika*, 63(3):581, 12 1976. ISSN 00063444. doi: 10.2307/2335739.

[22] Stef van Buuren. *Flexible Imputation of Missing Data, Second Edition*. Chapman and Hall/CRC, 7 2018. doi: 10.1201/9780429492259.

[23] Scott M Lundberg and Su-In Lee. A Unified Approach to Interpreting Model Predictions. In I Guyon, U V Luxburg, S Bengio, H Wallach, R Fergus, S Vishwanathan, and R Garnett, editors, *Advances in Neural Information Processing Systems 30*, pages 4765–4774. Curran Associates, Inc., 2017. URL <http://papers.nips.cc/paper/7062-a-unified-approach-to-interpreting-model-predictions.pdf>.

[24] Christoph Molnar. *Interpretable Machine Learning*. 2019.

[25] Been Kim, Rajiv Khanna, and Oluwasanmi O Koyejo. Examples are not enough, learn to criticize! Criticism for Interpretability. In D D Lee, M Sugiyama, U V Luxburg, I Guyon, and R Garnett, editors, *Advances in Neural Information Processing Systems 29*, pages 2280–2288. Curran Associates, Inc., 2016.

[26] Karthik S. Gurumoorthy, Amit Dhurandhar, Guillermo Cecchi, and Charu Aggarwal. Efficient Data Representation by Selecting Prototypes with Importance Weights. *Proceedings - IEEE International Conference on Data Mining, ICDM*, 2019-November:260–269, 7 2017. URL <http://arxiv.org/abs/1707.01212>.

[27] Ramprasaath R. Selvaraju, Michael Cogswell, Abhishek Das, Ramakrishna Vedantam, Devi Parikh, and Dhruv Batra. Grad-CAM: Visual Explanations from Deep Networks via Gradient-Based Localization. In *Proceedings of the IEEE International Conference on Computer Vision*, volume 2017-October, pages 618–626. Institute of Electrical and Electronics Engineers Inc., 12 2017. ISBN 9781538610329. doi: 10.1109/ICCV.2017.74.

[28] Umang Bhatt, Pradeep Ravikumar, and Jose M. F. Moura. Towards Aggregating Weighted Feature Attributions. *arXiv*, 1 2019. URL <http://arxiv.org/abs/1901.10040>.

[29] Mukund Sundararajan, Ankur Taly, and Qiqi Yan. Axiomatic Attribution for Deep Networks. In *Proceedings of the 34th International Conference on Machine Learning - Volume 70*, ICML'17, pages 3319–3328. JMLR.org, 2017.

[30] Oscar Li, Hao Liu, Chaofan Chen, and Cynthia Rudin. Deep Learning for Case-Based Reasoning through Prototypes: A Neural Network that Explains Its Predictions. *32nd AAAI Conference on Artificial Intelligence, AAAI 2018*, pages 3530–3537, 10 2017. URL <http://arxiv.org/abs/1710.04806>.

[31] Rishabh Agarwal, Nicholas Frosst, Xuezhou Zhang, Rich Caruana, and Geoffrey E. Hinton. Neural Additive Models: Interpretable Machine Learning with Neural Nets. *arXiv*, 4 2020. URL <http://arxiv.org/abs/2004.13912>.

[32] Harsha Nori, Samuel Jenkins, Paul Koch, and Rich Caruana. InterpretML: A Unified Framework for Machine Learning Interpretability. 9 2019. URL <http://arxiv.org/abs/1909.09223>.

[33] Yin Lou, Rich Caruana, Johannes Gehrke, and Giles Hooker. Accurate intelligible models with pairwise interactions. In *Proceedings of the ACM SIGKDD International Conference on Knowledge Discovery and Data Mining*, volume Part F128815, pages 623–631. Association for Computing Machinery, 8 2013. ISBN 9781450321747. doi: 10.1145/2487575.2487579.

[34] Dheeru Dua and Casey Graff. UCI Machine Learning Repository, 2017. URL <http://archive.ics.uci.edu/ml>.

[35] Yann LeCun, Léon Bottou, Yoshua Bengio, and Patrick Haffner. Gradient-based learning applied to document recognition. *Proceedings of the IEEE*, 86(11):2278–2323, 1998. ISSN 00189219. doi: 10.1109/5.726791.

[36] Yuval Netzer, Tao Wang, Adam Coates, Alessandro Bissacco, Bo Wu, and Andrew Y Ng. Reading digits in natural images with unsupervised feature learning. 2011.

[37] P Welinder, S Branson, T Mita, C Wah, F Schroff, S Belongie, and P Perona. Caltech-UCSD Birds 200. Technical Report CNS-TR-2010-001, California Institute of Technology, 2010.

[38] Xiang Zhang, Junbo Zhao, and Yann LeCun. Character-Level Convolutional Networks for Text Classification. In *Proceedings of the 28th International Conference on Neural Information Processing Systems - Volume 1*, NIPS'15, pages 649–657, Cambridge, MA, USA, 2015. MIT Press.

[39] Andrew L Maas, Raymond E Daly, Peter T Pham, Dan Huang, Andrew Y Ng, and Christopher Potts. Learning Word Vectors for Sentiment Analysis. In *Proceedings of the 49th Annual Meeting of the Association for Computational Linguistics: Human Language Technologies*, pages 142–150, Portland, Oregon, USA, 6 2011. Association for Computational Linguistics. URL <https://www.aclweb.org/anthology/P11-1015>.

[40] Ekin D Cubuk, Barret Zoph, Jonathon Shlens, and Quoc V Le. RandAugment: Practical Automated Data Augmentation with a Reduced Search Space. Technical report, 2020.

[41] P. McCullagh and J.A. Nelder. *Generalized Linear Models*. Number 2. Routledge, 1 2019. ISBN 9780203753736. doi: 10.1201/9780203753736. URL <https://www.taylorfrancis.com/books/9781351445856>.

[42] Leo Breiman. Random forests. *Machine Learning*, 45(1):5–32, 10 2001. ISSN 08856125. doi: 10.1023/A:1010933404324. URL <https://link.springer.com/article/10.1023/A:1010933404324>.

[43] Kaiming He, Xiangyu Zhang, Shaoqing Ren, and Jian Sun. Deep residual learning for image recognition. In *Proceedings of the IEEE Computer Society Conference on Computer Vision and Pattern Recognition*, volume 2016-December, pages 770–778. IEEE Computer Society, 12 2016. ISBN 9781467388504. doi: 10.1109/CVPR.2016.90. URL <http://image-net.org/challenges/LSVRC/2015/>.

[44] Zhengyang Wang, Xia Hu, and Shuiwang Ji. iCapsNets: Towards Interpretable Capsule Networks for Text Classification, 1 2020.

[45] Ju He, Jie-Neng Chen, Shuai Liu, Adam Kortylewski, Cheng Yang, Yutong Bai, Changhu Wang, and Alan Yuille. TransFG: A Transformer Architecture for Fine-grained Recognition. 3 2021. URL <http://arxiv.org/abs/2103.07976>.

[46] Alexey Dosovitskiy, Lucas Beyer, Alexander Kolesnikov, Dirk Weissenborn, Xiaohua Zhai, Thomas Unterthiner, Mostafa Dehghani, Matthias Minderer, Georg Heigold, Sylvain Gelly, Jakob Uszkoreit, and Neil Houlsby. An Image is worth 16X16 words: Transformers for Image Recognition at Scale. In *ICLR*, 9 2021.

[47] Adam Byerly, Tatiana Kalganova, and Ian Dear. A Branching and Merging Convolutional Network with Homogeneous Filter Capsules. 1 2020. URL <http://arxiv.org/abs/2001.09136>.

[48] Sepp Hochreiter and Jürgen Schmidhuber. Long Short-Term Memory. *Neural Computation*, 9(8):1735–1780, 11 1997. ISSN 08997667. doi: 10.1162/neco.1997.9.8.1735. URL <https://dl.acm.org/doi/abs/10.1162/neco.1997.9.8.1735>.

[49] Baoxin Wang. Disconnected recurrent neural networks for text categorization. In *ACL 2018 - 56th Annual Meeting of the Association for Computational Linguistics, Proceedings of the Conference (Long Papers)*, volume 1, pages 2311–2320. Association for Computational Linguistics (ACL), 2018. ISBN 9781948087322. doi: 10.18653/v1/p18-1215. URL <https://www.aclweb.org/anthology/P18-1215>.

[50] Andrew M. Dai and Quoc V. Le. Semi-supervised Sequence Learning. *Advances in Neural Information Processing Systems*, 2015-January:3079–3087, 11 2015. URL <http://arxiv.org/abs/1511.01432>.

[51] Alexis Conneau, Holger Schwenk, Yann Le Cun, and Loïc Boite Barrau. Very Deep Convolutional Networks for Text Classification. Technical report, 2017. URL <https://www.aclweb.org/anthology/E17-1104>.

[52] Jader Abreu, Luis Fred, David Macêdo, and Cleber Zanchettin. Hierarchical Attentional Hybrid Neural Networks for Document Classification. In *Lecture Notes in Computer Science (including subseries Lecture Notes in Artificial Intelligence and Lecture Notes in Bioinformatics)*, volume 11731 LNCS, pages 396–402. Springer Verlag, 2019. ISBN 9783030304928. doi: 10.1007/978-3-030-30493-5{_}39.

[53] Zhilin Yang, Zihang Dai, Yiming Yang, Jaime Carbonell, Ruslan Salakhutdinov, and Quoc V. Le. XLNet: Generalized Autoregressive Pretraining for Language Understanding. *Advances in Neural Information Processing Systems*, 32, 6 2019. URL <http://arxiv.org/abs/1906.08237>.

[54] Olga Russakovsky, Jia Deng, Hao Su, Jonathan Krause, Sanjeev Satheesh, Sean Ma, Zhiheng Huang, Andrej Karpathy, Aditya Khosla, Michael Bernstein, Alexander C. Berg, and Li Fei-Fei. ImageNet Large Scale Visual Recognition Challenge. *International Journal of Computer Vision*, 115(3):211–252, 9 2014. URL <http://arxiv.org/abs/1409.0575>.

[55] Saining Xie, Ross Girshick, Piotr Dollár, Zhuowen Tu, and Kaiming He. Aggregated residual transformations for deep neural networks. In *Proceedings of the IEEE conference on computer vision and pattern recognition*, pages 1492–1500, 2017.

[56] Karen Simonyan, Andrea Vedaldi, and Andrew Zisserman. Deep inside convolutional networks: Visualising image classification models and saliency maps. *arXiv preprint arXiv:1312.6034*, 2013.

[57] Pieter-Jan Kindermans, Kristof Schütt, Klaus-Robert Müller, and Sven Dähne. Investigating the influence of noise and distractors on the interpretation of neural networks. 11 2016. URL <http://arxiv.org/abs/1611.07270>.

[58] Matthew D. Zeiler and Rob Fergus. Visualizing and understanding convolutional networks. In *Lecture Notes in Computer Science (including subseries Lecture Notes in Artificial Intelligence and Lecture Notes in Bioinformatics)*, volume 8689 LNCS, pages 818–833. Springer Verlag, 11 2014. ISBN 9783319105895. doi: 10.1007/978-3-319-10590-1{_}53. URL <https://arxiv.org/abs/1311.2901v3>.

[59] Thomas M Cover and Joy A Thomas. *Elements of Information Theory (Wiley Series in Telecommunications and Signal Processing)*. Wiley-Interscience, USA, 2006. ISBN 0471241954.

[60] Oliver Eberle, Jochen Buttner, Florian Krautli, Klaus-Robert Muller, Matteo Valleriani, and Gregoire Montavon. Building and Interpreting Deep Similarity Models. *IEEE Transactions on Pattern Analysis and Machine Intelligence*, (01):1–1, 9 2020. ISSN 0162-8828. doi: 10.1109/tpami.2020.3020738.

[61] Rainer E. Burkard and Eranda Çela. Linear Assignment Problems and Extensions. In *Handbook of Combinatorial Optimization*, pages 75–149. Springer US, 1999. doi: 10.1007/978-1-4757-3023-4{_}2. URL https://link.springer.com/chapter/10.1007/978-1-4757-3023-4_2.

[62] Tim Miller. Explanation in artificial intelligence: Insights from the social sciences, 2 2019. ISSN 00043702.

[63] Johanes Schneider and Joshua Handali. Personalized explanation in machine learning. 1 2019. URL <http://arxiv.org/abs/1901.00770>.

[64] Kacper Sokol and · Peter Flach. One Explanation Does Not Fit All The Promise of Interactive Explanations for Machine Learning Transparency. *KI - Künstliche Intelligenz*, 34:3. doi: 10.1007/s13218-020-00637-y. URL <https://doi.org/10.1007/s13218-020-00637-y>.

[65] Kay I. Penny and Ian Atkinson. Approaches for dealing with missing data in health care studies. *Journal of Clinical Nursing*, 21(19-20):2722–2729, 10 2012. ISSN 09621067. doi: 10.1111/j.1365-2702.2011.03854.x. URL <https://pubmed.ncbi.nlm.nih.gov/21895816/>.

[66] Brian J. Wells, Amy S. Nowacki, Kevin Chagin, and Michael W. Kattan. Strategies for Handling Missing Data in Electronic Health Record Derived Data. *eGEMs (Generating Evidence & Methods to improve patient outcomes)*, 1(3):7, 12 2013. ISSN 2327-9214. doi: 10.13063/2327-9214.1035. URL [/pmc/articles/PMC4371484/](https://pmc/articles/PMC4371484/)?report=abstract&url=https://www.ncbi.nlm.nih.gov/pmc/articles/PMC4371484/.

[67] Olawale F. Ayilara, Lisa Zhang, Tolulope T. Sajobi, Richard Sawatzky, Eric Bohm, and Lisa M. Lix. Impact of missing data on bias and precision when estimating change in patient-reported outcomes from a clinical registry. *Health and Quality of Life Outcomes*, 17(1):1–9, 6 2019. ISSN 14777525. doi: 10.1186/s12955-019-1181-2. URL <https://doi.org/10.1186/s12955-019-1181-2>.

[68] Srinidhi Hiriyannaiah, Siddesh G. M., Mumtaz Irteqa Ahmed, Kolli Saivenu, Anant Raj, K. G. Srinivasa, and L. M. Patnaik. Multi-modal Data-Driven Analytics for Health Care. pages 139–155. Springer, Singapore, 2021. doi: 10.1007/978-981-16-0415-7{_}7. URL https://link.springer.com/10.1007/978-981-16-0415-7_7.

[69] Alfredo Vellido. The importance of interpretability and visualization in machine learning for applications in medicine and health care. *Neural Computing and Applications*, 32(24):18069–18083, 12 2020. ISSN 14333058. doi: 10.1007/s00521-019-04051-w. URL <https://doi.org/10.1007/s00521-019-04051-w>.

[70] Diederik P. Kingma and Jimmy Lei Ba. Adam: A method for stochastic optimization. In *3rd International Conference on Learning Representations, ICLR 2015 - Conference Track Proceedings*. International Conference on Learning Representations, ICLR, 12 2015. URL <https://arxiv.org/abs/1412.6980v9>.

[71] Ilya Loshchilov and Frank Hutter. Decoupled Weight Decay Regularization. *7th International Conference on Learning Representations, ICLR 2019*, 11 2017. URL <http://arxiv.org/abs/1711.05101>.

[72] Liyuan Liu, Haoming Jiang, Pengcheng He, Weizhu Chen, Xiaodong Liu, Jianfeng Gao, and Jiawei Han. On the Variance of the Adaptive Learning Rate and Beyond. In *Proceedings of the Eighth International Conference on Learning Representations (ICLR 2020)*, 4 2020.

[73] Ilya Loshchilov and Frank Hutter. SGDR: Stochastic Gradient Descent with Warm Restarts. *5th International Conference on Learning Representations, ICLR 2017 - Conference Track Proceedings*, 8 2016. URL <http://arxiv.org/abs/1608.03983>.

Checklist

The checklist follows the references. Please read the checklist guidelines carefully for information on how to answer these questions. For each question, change the default [TODO] to [Yes] , [No] , or [N/A] . You are strongly encouraged to include a **justification to your answer**, either by referencing the appropriate section of your paper or providing a brief inline description. For example:

- Did you include the license to the code and datasets? [Yes] See Section ??.
- Did you include the license to the code and datasets? [No] The code and the data are proprietary.
- Did you include the license to the code and datasets? [N/A]

Please do not modify the questions and only use the provided macros for your answers. Note that the Checklist section does not count towards the page limit. In your paper, please delete this instructions block and only keep the Checklist section heading above along with the questions/answers below.

1. For all authors...
 - (a) Do the main claims made in the abstract and introduction accurately reflect the paper's contributions and scope? [Yes]
 - (b) Did you describe the limitations of your work? [Yes]
 - (c) Did you discuss any potential negative societal impacts of your work? [No] As our work proposes a way to make traditionally black-box models more transparent, we do not foresee any obvious negative impact.
 - (d) Have you read the ethics review guidelines and ensured that your paper conforms to them? [Yes]
2. If you are including theoretical results...
 - (a) Did you state the full set of assumptions of all theoretical results? [N/A]
 - (b) Did you include complete proofs of all theoretical results? [N/A]
3. If you ran experiments...
 - (a) Did you include the code, data, and instructions needed to reproduce the main experimental results (either in the supplemental material or as a URL)? [Yes] In the appendix
 - (b) Did you specify all the training details (e.g., data splits, hyperparameters, how they were chosen)? [Yes] In the appendix
 - (c) Did you report error bars (e.g., with respect to the random seed after running experiments multiple times)? [Yes] but not in the main texts. Where applicable the information will be reported in the appendix
 - (d) Did you include the total amount of compute and the type of resources used (e.g., type of GPUs, internal cluster, or cloud provider)? [No] As our work is currently on making deep learning models interpretable, our results are focused on interpretability and approximation capacity, and not (yet) on the computational resources needed.
4. If you are using existing assets (e.g., code, data, models) or curating/releasing new assets...
 - (a) If your work uses existing assets, did you cite the creators? [Yes]
 - (b) Did you mention the license of the assets? [N/A]
 - (c) Did you include any new assets either in the supplemental material or as a URL? [N/A]
 - (d) Did you discuss whether and how consent was obtained from people whose data you're using/curating? [N/A]
 - (e) Did you discuss whether the data you are using/curating contains personally identifiable information or offensive content? [N/A]
5. If you used crowdsourcing or conducted research with human subjects...
 - (a) Did you include the full text of instructions given to participants and screenshots, if applicable? [N/A]

- (b) Did you describe any potential participant risks, with links to Institutional Review Board (IRB) approvals, if applicable? [N/A]
- (c) Did you include the estimated hourly wage paid to participants and the total amount spent on participant compensation? [N/A]

A Training details

All the deep learning models were trained using Adam [70] (or variants thereof, i.e. AdamW [71], RAdam [72]). Learning rates varied in the set $\{0.001, 0.0005, 0.0001, 0.00005\}$. Training was tested with no learning rate scheduling, as well as exponential decay, step decay, and cosine annealing [73] (with and without restart). The chosen hyperparameters for each experiment can be retrieved from the corresponding `config.json` file provided in the accompanying code. Details about the architectures used are also provided in the accompanying code.

Tabular datasets. For each datasets, 10 different runs are performed. Table 1a reports means among these runs. In Table 2a we report again the mean, together with standard deviation and top performance (max).

Image datasets. For each datasets, 5 different runs are performed (with the best set of hyperparameters). Table 1b reports top performance among these runs. In Table 2b we report again the top performance (max), together with the mean among the 5 runs, and standard deviation.

Text datasets. For each datasets, 5 different runs are performed (with the best set of hyperparameters). Table 1c reports top performance among these runs. In Table 2c we report again the top performance (max), together with the mean among the 5 runs, and standard deviation.

B Further results

B.1 Performance results

Here we report more detailed performance results (Table 2). The experimental setup is reported in the previous section A. Note that the inconsistencies in the results between Table 1 and Table 2 are due to the fact that new experiments have been run with *not* fixed random seeds to produce Table 2. However, this change does not affect the interpretation of the results discussed in Section 4.1.

Table 2: Further benchmarking results. (*) denotes pretrained models or models using automated augmentation strategies. (**) denotes FLAN models that use pretrained models as *part* of the feature functions. Reporting mean (max) \pm standard deviation over 10 runs for tabular datasets, and 5 runs for the other datasets.

(a) Area under the curve (AUC) on tabular datasets.

	COMPAS	adult	heart	mammo
Logistic Regression [41]	0.905 (0.917) ± 0.006	0.892 (0.896) ± 0.003	0.873 (0.923) ± 0.032	0.841 (0.874) ± 0.017
Decision Tree (small) [10]	0.903 (0.915) ± 0.007	0.865 (0.871) ± 0.005	0.849 (0.882) ± 0.026	0.799 (0.818) ± 0.017
Decision Tree (unrestricted) [10]	0.902 (0.915) ± 0.007	0.813 (0.821) ± 0.005	0.848 (0.882) ± 0.024	0.801 (0.826) ± 0.016
Random Forest[42]	0.915 (0.927) ± 0.007	0.869 (0.877) ± 0.004	0.945 (0.964) ± 0.014	0.822 (0.841) ± 0.016
EBM [32]	0.911 (0.923) ± 0.008	0.893 (0.896) ± 0.002	0.941 (0.959) ± 0.015	0.840 (0.869) ± 0.015
MLP	0.915 (0.927) ± 0.006	0.874 (0.883) ± 0.005	0.937 (0.958) ± 0.023	0.831 (0.856) ± 0.014
SENN [12]	0.910 (0.922) ± 0.007	0.865 (0.873) ± 0.005	0.881 (0.925) ± 0.036	0.834 (0.860) ± 0.013
FLAN	0.914 (0.923) ± 0.004	0.880 (0.886) ± 0.004	0.950 (0.973) ± 0.019	0.832 (0.867) ± 0.019

(b) Test accuracy (%) on image datasets.

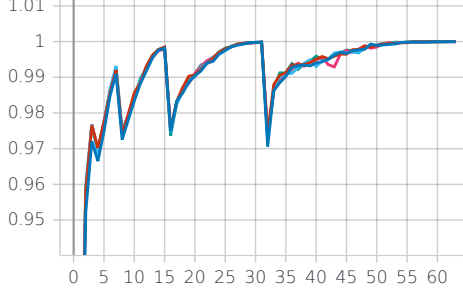
	MNIST	SVHN	CUB
ResNet [43, 44, 45]	99.2	94.5*	84.5*
iCaps [44]	99.2	92.0	-
ViT [45, 46]	-	88.9	90.4*
ProtoPNet [11]	-	-	84.8*
SENN [12]	99.1	-	-
SotA [40, 45, 47]	99.84	99.0*	91.3*
	99.00 (99.05) ± 0.0007	93.37 (93.41) ± 0.0004	71.17 (71.53) ± 0.003

(c) Test accuracy (%) on text datasets.

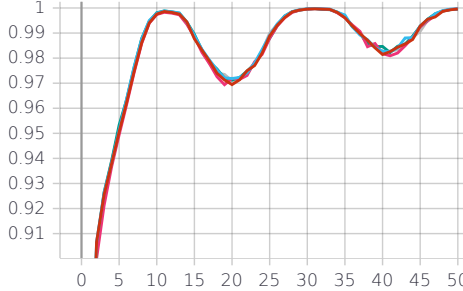
	AGNews	IMDb
CharCNN [38]	90.49	-
LSTM [48, 49, 50]	93.8	86.5
VDCNN [51, 52]	91.33	79.47
HAHNN [52]	-	95.17
XLNet [53]	95.6*	96.8*
	90.6 (90.9) ± 0.003	84.9 (85.1) ± 0.002

B.1.1 Training graphs

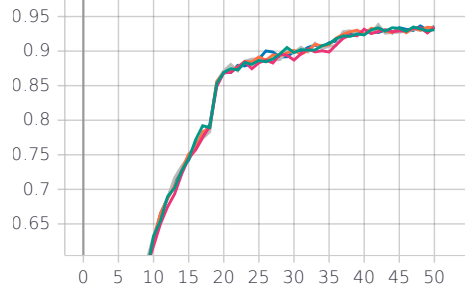
In Section 4.1 and Section B.1 we reported the best models in terms of *test* performance. Here we report (Figure 6) the training curves of some models that achieved 100% (resp. 94%) training accuracy on MNIST, AGNews, and IMDB (resp. CUB), but generalised poorly.



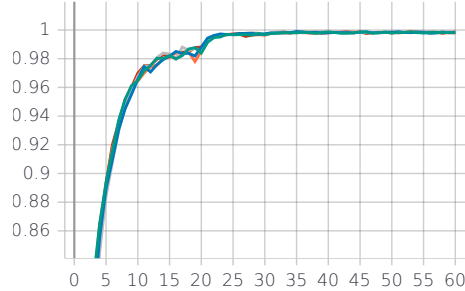
(a) Training graphs for the MNIST dataset for 5 experiments (top *train* performance 100%).



(c) Training graphs for the AGNews dataset for 5 experiments (top *train* performance 100%).



(b) Training graphs for the CUB dataset for 5 experiments (top *train* performance 94%).



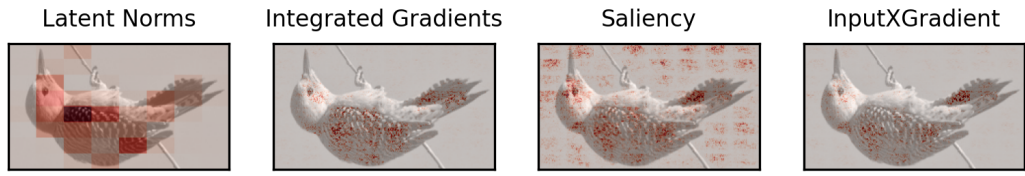
(d) Training graphs for the IMDB dataset for 5 experiments (top *train* performance 100%).

Figure 6: Training graphs for various experiments.

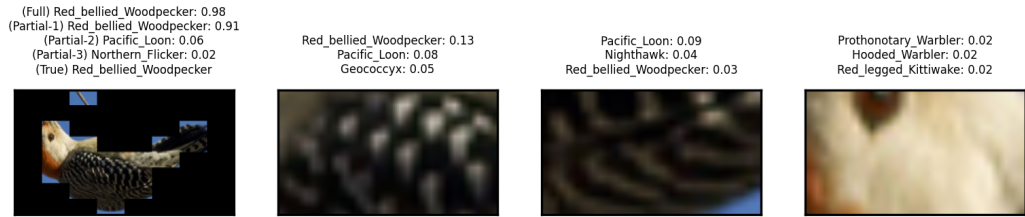
B.2 Interpretability results

B.2.1 CUB

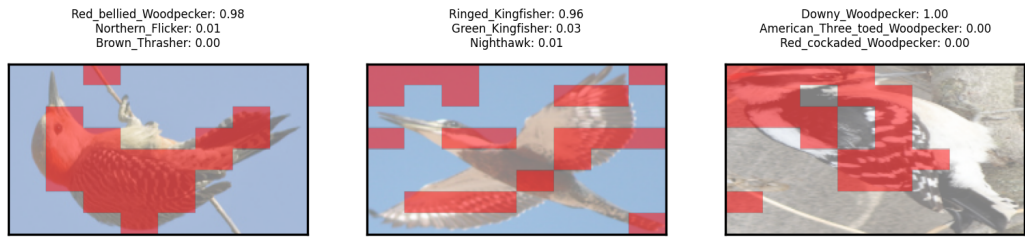
Here we show more interpretability results from the CUB dataset.



(a) Feature attribution comparisons.

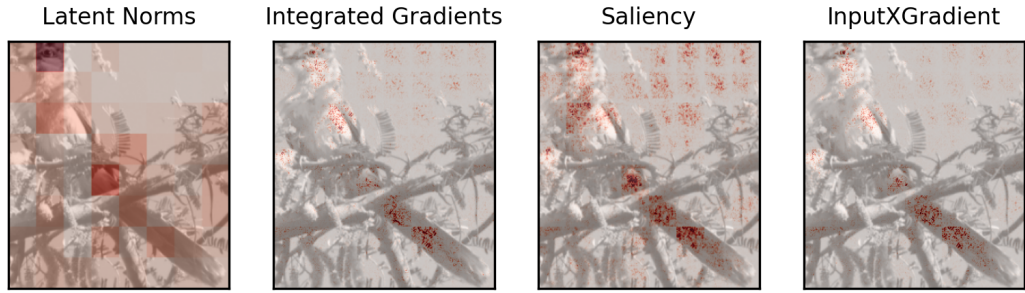


(b) Algorithmic interpretation.



(c) Example-based interpretation with correspondences.

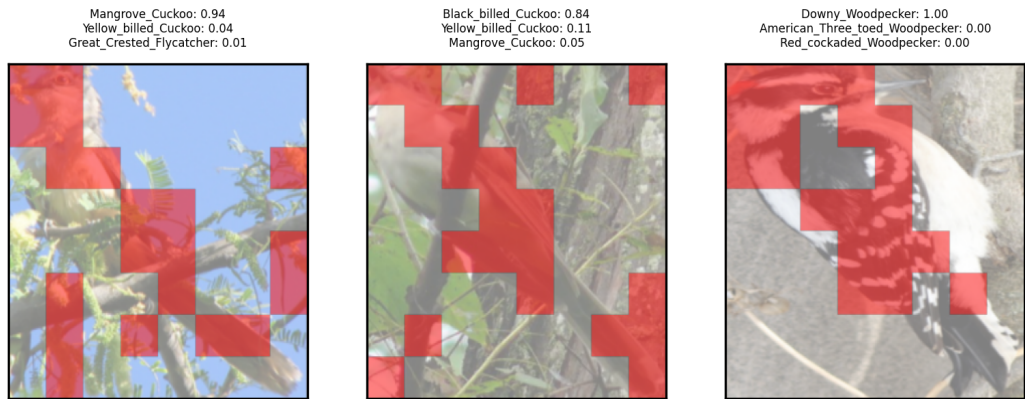
Figure 7: Additional interpretability results.



(a) Feature attribution comparisons.

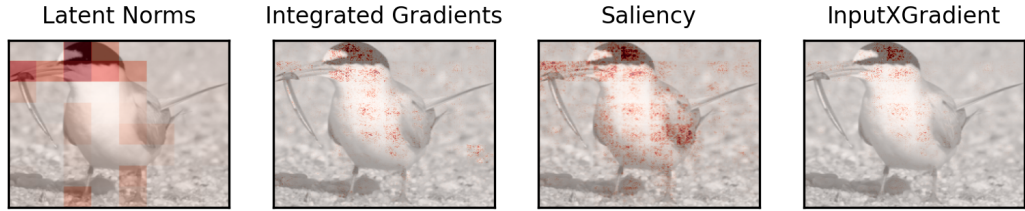


(b) Algorithmic interpretation.

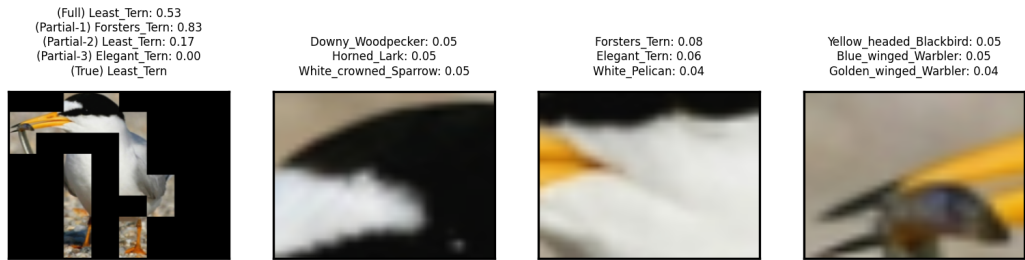


(c) Example-based interpretation with correspondences.

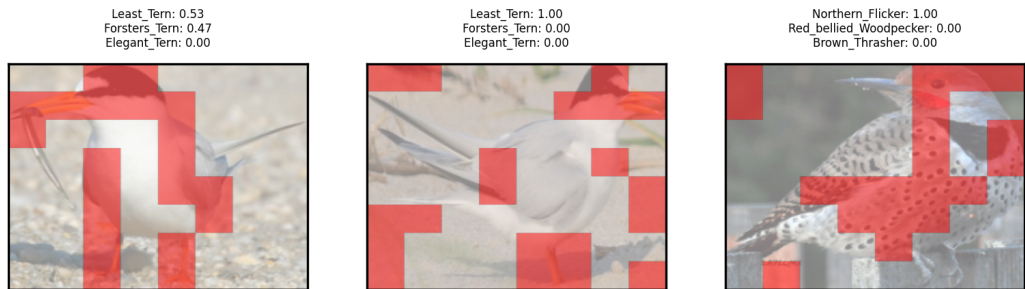
Figure 8: Additional interpretability results.



(a) Feature attribution comparisons.

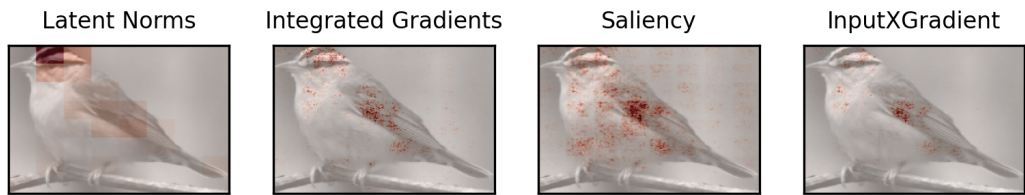


(b) Algorithmic interpretation.



(c) Example-based interpretation with correspondences.

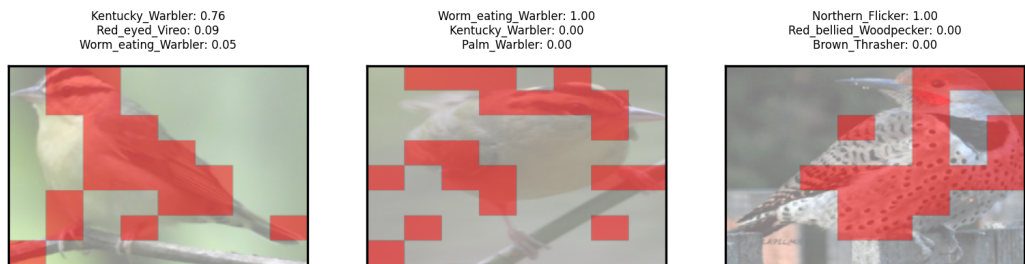
Figure 9: Additional interpretability results.



(a) Feature attribution comparisons.



(b) Algorithmic interpretation.



(c) Example-based interpretation with correspondences.

Figure 10: Additional interpretability results.

C Supplemental files

Config files and checkpoints of trained models are available at https://drive.google.com/file/d/1JG6Ck0Dhm7wI_NwFXW_pV20V4vPqnNVp/view?usp=sharing .